# $NiAl_3$ formation in Al/Ni thin-film bilayers with and without contamination

E. Ma and M-A. Nicolet
*California Institute of Technology, 116-81, Pasadena, California 91125*

M. Nathan[a)]
*Martin Marietta Laboratories, 1450 South Rolling Road, Baltimore, Maryland 21227*

(Received 26 August 1988; accepted for publication 6 November 1988)

The interfacial reactions induced by vacuum furnace annealing and rapid thermal annealing in sequentially deposited Al/Ni bimetallic thin-film diffusion couples have been investigated with MeV $^4He^+$ backscattering spectrometry, cross-sectional transmission electron microscopy, and Auger electron spectroscopy. Upon annealing, $NiAl_3$ is the first aluminide phase to grow. In uncontaminated samples, the $NiAl_3$ growth proceeds in uniform planar fashion, governed by diffusion-limited kinetics. The kinetics data fit well with those for $NiAl_3$ growth on large-grained Al substrates, yielding a common kinetics law of $x^2 = kt$, where $x$ is the thickness of the $NiAl_3$ grown at the interface, $t$ is the annealing duration, and $k$ is the growth constant, which is given by $k = 2.24(\mathrm{cm}^2/\mathrm{s})\exp(-1.5 \pm 0.1\ \mathrm{eV}/k_B T)$, in which $T$ is the annealing temperature and $k_B$ is the Boltzmann constant. Microscopic examination reveals slight nonuniformity at the Al/$NiAl_3$ interface resulting from shallow local protrusions of $NiAl_3$ grains into the Al layer at grain boundaries. When either the Al film or the Al/Ni interface is purposely contaminated during sample preparation, the roughness at this Al/$NiAl_3$ interface becomes very pronounced, and the reaction rate is significantly reduced. Meanwhile, Ni motion becomes appreciable as $NiAl_3$ grains and/or Ni severely penetrate the Al layer. In contrast, the $NiAl_3$/Ni interface remains sharp in all samples. The irregular morphology and nonuniform reaction cannot be attributed uniquely to the presence of grain boundaries in the Al film, but rather are a combined effect of impurities and Al grain boundaries. Short-term rapid thermal annealing at elevated temperatures appreciably alleviates the nonuniformity at the Al/$NiAl_3$ interface in contaminated samples.

## I. INTRODUCTION

The interaction between thin films of Al and transition metals has attracted wide attention in recent years.[1] Knowledge of such reactions upon thermal treatment is of practical importance to applications in metallization schemes in integrated circuits,[2] and is of intrinsic interest to the field of thin-film and interface studies in its own right.[3] For contact metallization applications, it would be desirable to have a single compound at the Al/metal interface that has uniform growth with well-defined kinetics. The Al-Ni thin-film reaction, in particular, merits attention because of conflicting observations. Reproducible kinetics of $NiAl_3$ growth were obtained for the first time in our previous work with Ni on large-grained Al substrates.[4,5] Complications arise, however, when thin-film Al substrates are used. Upon furnace annealing, such Al/Ni thin-film bilayers tend to suffer from severe Ni penetration along the Al grain boundaries.[5] Although an irregular Al-Ni reaction with pronounced nonuniformity was reported as early as the mid-1970's,[3,6] uniform $NiAl_3$ formation was also found in Al/Ni thin-film reaction without using large-grained Al substrates.[7–9] These contradictory facts point to unrecognized sensitive factors which vary during sample preparation and/or subsequent thermal treatment and appreciably affect the outcome. To provide further insight into this issue, we have undertaken an extended investigation on $NiAl_3$ growth in evaporated Al/Ni thin films. As impurities are known to be responsible for many observed inconsistencies in thin-film reactions, parallel experiments were carried out in samples with and without intentional contamination.

## II. EXPERIMENTAL PROCEDURES

Bilayers of Al/Ni were prepared by sequential *e*-beam evaporation of Al and Ni, in that order, onto thermally oxidized ⟨111⟩ or ⟨100⟩ Si substrates. The depositions were performed in an oil-free evaporation unit evacuated to a base pressure of $<5\times10^{-8}$ Torr. The working pressure increased to $(1–4)\times10^{-7}$ Torr during evaporation. Some samples were purposely contaminated during deposition in various ways, as will be described separately in later sections. Furnace annealing was carried out in a vacuum of $(4–8)\times10^{-7}$ Torr, and rapid thermal annealing (RTA) was performed in ultrapure (99.999%) argon. The furnace annealing temperatures were carefully calibrated and were accurate to within $\pm$ 2 °C. The RTA temperature, on the other hand, is only nominal due to the uncertainty in its measurement. The interfacial reaction in every annealed sample was monitored by 2-MeV $^4He^+$ backscattering spectrometry (BS). Some samples were also examined by cross-sectional transmission electron microscopy (XTEM), or by Auger electron spectroscopy (AES), which complemented the BS analysis and was employed to probe for light impurity species. Glancing angle x-ray diffraction (Read camera) and electron diffraction were used for occasional phase identification.

[a)] Present address: Department of Electronic Materials and Devices, Tel Aviv University, Ramat Aviv, Israel.

 0021-8979/89/072703-06$02.40  

## III. RESULTS

### A. Growth kinetics of $NiAl_3$

The data for the clean Al/Ni thin-film samples without intentional contamination are presented first. The as-deposited bilayer has the configuration of 180-nm Ni on 470-nm Al. Shown in Fig. 1 is a group of superimposed BS spectra for samples furnace annealed at 324 °C for various durations. The basic feature of these spectra is the progressive thickening of a well-defined compound in a laterally uniform fashion, the composition of which was determined from BS signal heights to be a fixed value of Ni:Al = 1:3 ± 5%. The $NiAl_3$ phase is also positively identified by x-ray diffraction (XRD) analysis.[10] The formation of $NiAl_3$ as the first growing phase in the Al/Ni reaction has been consistently reported by a number of authors.[3–9]

The planar growth of a single $NiAl_3$ phase permits the extraction of the formation kinetics of $NiAl_3$. The energy widths of the $NiAl_3$ steps in the BS spectra (Fig. 1) are converted into the compound thickness by assuming a bulk density of $1.707\times10^{22}$ $NiAl_3$ units/cm$^3$ for the orthorhombic $NiAl_3$ phase.[11] Figure 2 is thereby constructed, in which the squared thickness of $NiAl_3$ is plotted against the annealing duration. Straight lines are least-squares fitted to data points for each temperature. The perfect fits exhibited in the plot demonstrate a square-root growth law indicative of a transport-limited process. To ensure the reproducibility of the data additional samples were prepared with varied configurations, namely, either of Ni and Al layers of reduced thicknesses (100-nm Ni on 180-nm Al) or in reversed sequence, i.e., with Al on top (500-nm Al on 150-nm Ni). Simultaneous annealing of these samples at 292 °C gave the results displayed in Fig. 3. No significant discrepancies in reaction kinetics are noted from sample to sample.

The $NiAl_3$ growth rates deduced from Fig. 2 are presented in the Arrhenius plot of Fig. 4, along with the kinetics data on large-grained Al substrate (Ref. 5). It is evident that all the data points can be well represented by a common linear fit, as is done in Fig. 4 with a solid line. This means that

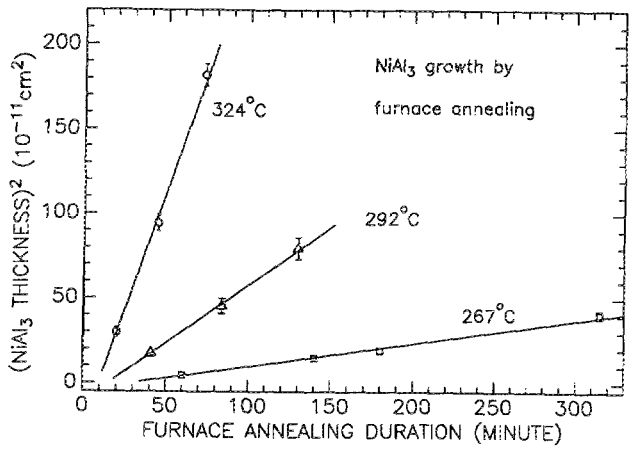


FIG. 2. The squared thickness of the growing layer of $NiAl_3$ vs annealing duration for three temperatures.

$NiAl_3$ grows at almost the same rate, presumably via the same mechanism irrespective of whether the Al substrate used is a thin film or a bulk material. Since the Al plate used in Ref. 5 is of high purity (99.999%), we interpret the consistency of the growth observed as an indication that our deposited Al films are free of deleterious contamination. For completeness, we also include in Fig. 4 the temperature dependence of $NiAl_3$ growth rates for bulk and lateral Al-$Ni_2Al_3$ diffusion couples summarized in Ref. 8a.

The kinetics law for $NiAl_3$ growth derived from Figs. 2 and 4 has the form of $x^2 = kt$, where $x$ is the thickness of the grown $NiAl_3$ compound, $t$ is the annealing duration, and $k$ is the growth constant given by $k = 2.24(\text{cm}^2/\text{s})\exp(-1.5\pm0.1\,\text{eV})/k_BT$, where $T$ is the annealing temperature and $k_B$ is the Boltzmann constant. This law holds for both evaporated and large-grained Al substrates in the temperature range of 250–400 °C.

Detailed features of the interfaces of a typical reacted sample are shown in the bright-field XTEM picture of Fig. 5. The $NiAl_3$/Ni interface is sharp and laterally uniform, whereas slight nonuniformities are visible at the Al/$NiAl_3$

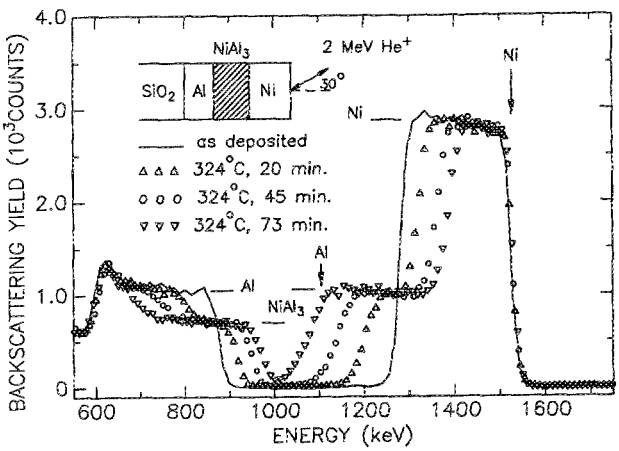


FIG. 1. 2-MeV $^4He^+$ backscattering spectra of Al/Ni samples annealed in a vacuum furnace at 324 °C for various durations showing the progressive planar growth of $NiAl_3$. The beam is incident 30° from the sample normal, and the detection angle is 170° with respect to the incident beam. This detection geometry is used to acquire all the spectra (except Fig. 12) shown in this paper.

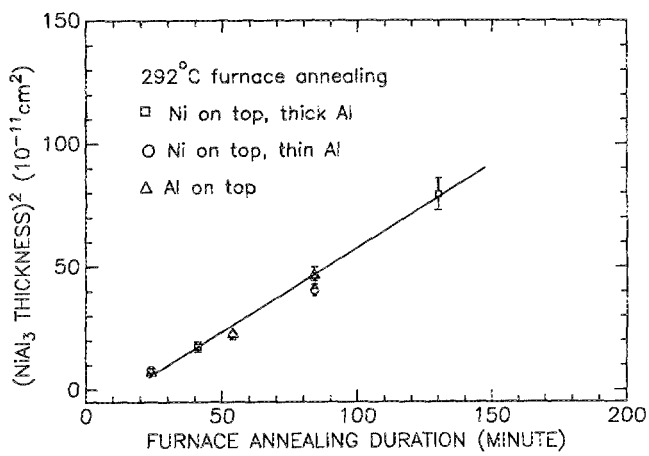


FIG. 3. Same plot as Fig. 2, but with three different sample configurations annealed at a fixed temperature 292 °C. The 292 °C data fit of Fig. 2 is reproduced with squares and the solid line. Additional data are added with circles and triangles. The consistency of the data verifies the reproducibility of the kinetics.

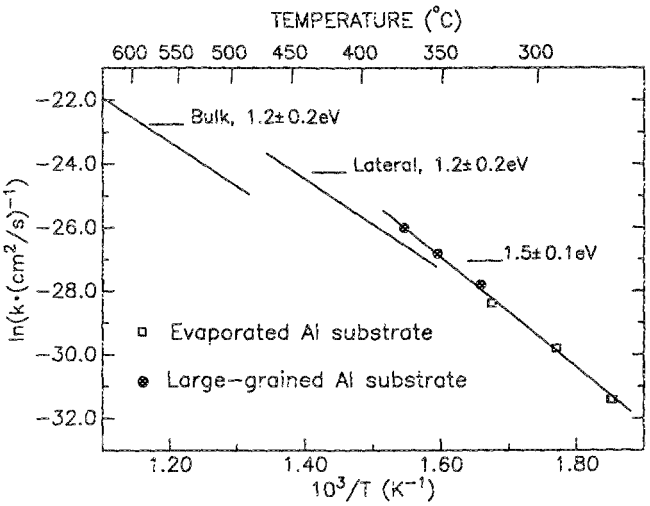


FIG. 4. Arrhenius plot of the $NiAl_3$ growth rates for Al/Ni thin-film bilayers (Fig. 2) as well as for Ni thin film on large-grained Al substrates (from Refs. 4 and 5). All the data points are least-squares fitted with a straight line, which yields a common activation energy of $1.5 \pm 0.1$ eV. Kinetics data for $NiAl_3$ growth in bulk and lateral Al-$Ni_2Al_3$ diffusion couples (from Ref. 8a) are also reproduced in the figure for completeness.

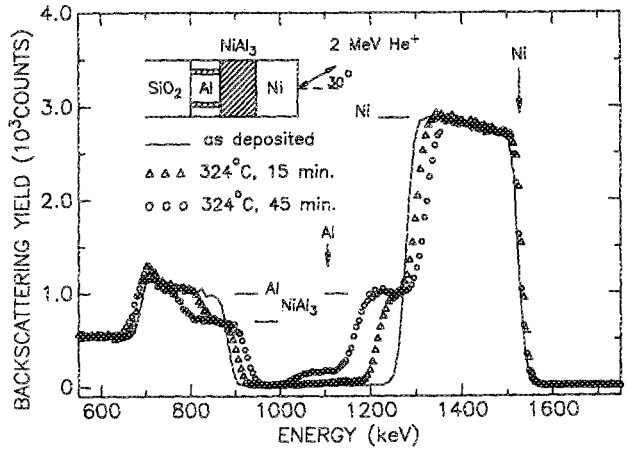


FIG. 6. 2-MeV $^4He^+$ backscattering spectra for furnace-annealed Al/Ni samples with contaminated Al film. A flat Ni tail develops at the back edge of the Ni signal in addition to a $NiAl_3$ step (compare with Fig. 1).

interface. There are occasional shallow protrusions of $NiAl_3$ grains into the Al layer, primarily at triple junctions that involve Al grain boundaries. These findings presumably account for the slightly sloped low-energy edges of Ni (or Al) signal at the $NiAl_3$ steps in the BS spectra.

Rapid thermal annealing of these Al/Ni bilayers leads basically to the same features of $NiAl_3$ growth in BS spectra. After inspecting and comparing a number or spectra, it is noticeable, although perhaps of secondary order, that the back trailing edges of the $NiAl_3$ steps appear steeper for RTA'd samples. The advantageous effect of RTA in improving the lateral uniformity at the Al/$NiAl_3$ interface will reemerge in the next few sections when we encounter rather irregular nonuniform reactions upon furnace annealing of contaminated samples.

### B. Contamination of Al film

A laterally nonuniform reaction behavior has been recorded by several previous experiments.[3–6] In view of the results presented in Sec. III A, it appears that the presence of Al grain boundaries by themselves does not necessarily lead to significant irregularities, as has been assumed by previous investigators.

Another factor that needs attention is the role of impurities which are known to have deleterious effects on thin-film reactions.[12–15] Thus, we investigated the influence of intentional contamination of the samples, starting with the Al layer. The Al and Ni films were again sequentially evaporated without breaking the vacuum. The Al, however, was deposited under a poor vacuum of about $8 \times 10^{-6}$ Torr instead of the normal $< 4 \times 10^{-7}$ Torr. Presented in Fig. 6 are the BS spectra of these samples as-deposited and annealed at 324 °C. A flat tail now appears at the back edge of the Ni signal together with a step corresponding to $NiAl_3$, suggesting movement of Ni into Al. The Ni tail could also be a result of local thickening of the Ni film, and/or Al migration into Ni, which would push Ni locally deep into the sample. However, these possibilities can be ruled out because (i) we do not see significant morphological changes in the Ni film or at its surface using TEM, and (ii) both BS spectra and TEM indicate a planar $NiAl_3$/Ni interface. An AES profile verifies that a Ni tail exists in Al at an overall concentration of about 4–5 at. % beyond the uniform layer of $NiAl_3$. Such a concentration is far above the solid solubility of Ni in Al, which is practically zero at low temperatures.[16] The Ni inside the Al layer is not seen under XTEM, probably because of its small amount. The XTEM pictures look similar to that shown in Fig. 5. We will come back to discuss the nature of the Ni buried in Al in the following sections.

Systematic identification of the compound phase was not undertaken for the contaminated samples described from this section on. We have taken the similarity of the BS spectra, namely, the frequent appearance of a step corresponding to $NiAl_3$ in the Ni and Al signals, as an indication that the compound formed is always $NiAl_3$. This identification was confirmed in one case by electron diffraction (Sec. III D).

It is still feasible to follow the growth of the $NiAl_3$ step along with annealing time in samples having a contaminated Al layer. The growth is again found to be transport-limited according to a $x^2$ vs $t$ plot (not shown). The $NiAl_3$ growth constant $k$ at 324 °C is about 45% of that of the clean samples. Very similar outcomes were described by Zhao *et al.* in Ref. 5 for thin-film Al/Ni bilayers, in which the $NiAl_3$

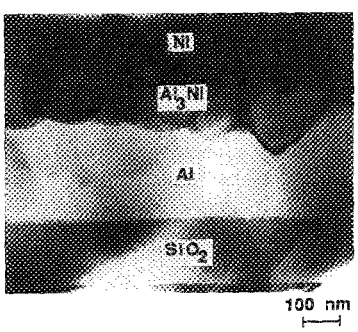


FIG. 5. Cross-sectional TEM bright-field image of a reacted Al/Ni sample (275 °C, 315 min). The $NiAl_3$/Ni interface is sharper than the Al/$NiAl_3$ interface. Note the occasional local protrusions of $NiAl_3$ grains into the unreacted Al layer.

growth rate was also found to be about half of that on the large-grained Al substrates. While Ref. 5 merely attributes the irregularities to Ni penetration into Al grain boundaries, we now have a clue that such a phenomenon relates to the presence of impurities during the deposition of the Al film.

Ni penetration is largely suppressed when RTA is employed. This is manifested in Fig. 7 where the $NiAl_3$ steps now look similar to those in Fig. 1 whereas the trailing Ni tail is diminished.

### C. Contamination of the Ni film

The Ni layer of some samples was contaminated in the same manner as described above for Al. The working vacuum during Ni evaporation was about $(2–4)\times10^{-6}$ Torr. The BS spectra of samples after furnace annealing at 324 °C closely resemble those shown in Fig. 1. There is a distinct $NiAl_3$ interlayer with uniform boundaries growing at the interface. The growth rate is slightly lower (by about 10%) than that for clean samples.

We also cite from Ref. 5 that a deliberate contamination, with a high evaporation pressure of $4\times10^{-6}$ Torr, of the Ni film overlain on large-grained Al substrates merely lowers the growth rate by 20%. The simple picture of planar $NiAl_3$ growth remained unaltered.

### D. Contamination at the interface

An oxide layer at the Al/Ni interface, when equivalent to or thicker than 4.5 nm, is known to completely block the Al-Ni reaction at 400 °C.[5] To further observe the effect of an interfacial barrier, we intentionally broke the vacuum after Al evaporation. The system was vented with air to 1 Torr for 10 min, and then pumped back down again for the Ni deposition. The interfacial barrier thus formed is presumably thinner than a native Al oxide layer which typically is about 3.5 nm thick.[12] BS spectra for such samples after furnace annealing are shown in Fig. 8. The Ni signal suggests that Ni first penetrates deeply and locally into Al, followed later by $NiAl_3$ growth at the Al/Ni interface. The Al/$NiAl_3$ interface is very rough, as inferred from a broad slanted trailing edge of the Ni signal. Al penetration into Ni also occurs, as evidence by a decrease in Ni signal height and a gray appearance of the sample surface. Figure 8 also contains signs of laterally nonuniform morphological rearrangements in the films.

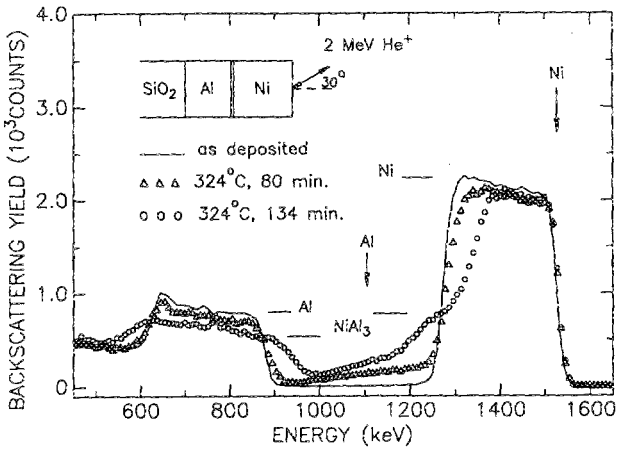


FIG. 8. 2-MeV $^4He^+$ backscattering spectra for Al/Ni samples with a contaminated original Al/Ni interface (see insert for the as-deposited sample; the double line at the interface represents a possible interfacial impurity barrier). Deep nonuniform interpenetration of Ni and Al is obvious.

It is of interest to tell whether the penetrating Ni is present in the form of protruding aluminide grains or simply dissolved in Al, e.g., in Al grain boundaries. Backscattering and AES, however, are unable to make such a distinction. Some insight in this respect can be provided by TEM examinations. A plane-view TEM sample was prepared from the

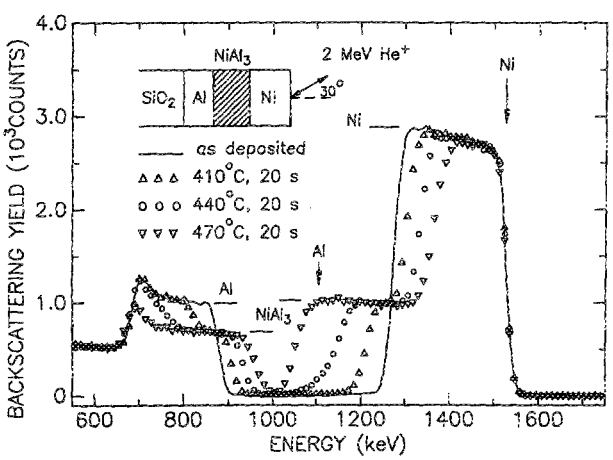


FIG. 7. 2-MeV $^4He^+$ backscattering spectra for Al/Ni samples with contaminated Al film (same as in Fig. 6) after RTA at various temperatures for 20 s. The Ni tail seen in Fig. 6 is now suppressed.

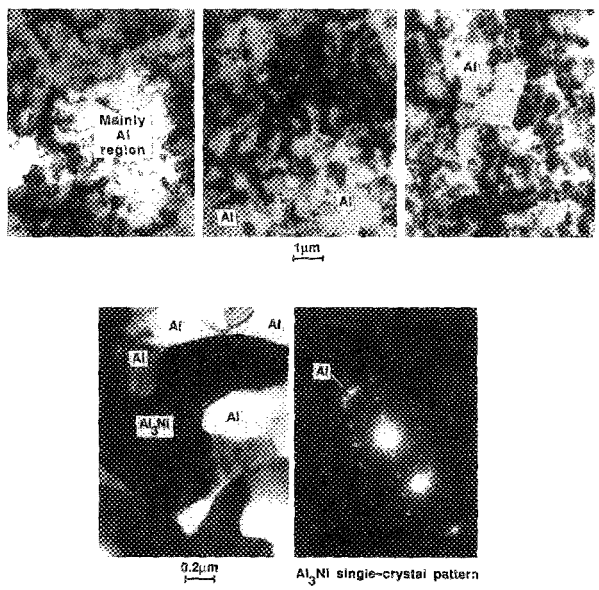


FIG. 9. Plane-view TEM of Al/Ni sample with contaminated original interface (same as in Fig. 8) annealed at 324 °C for 80 min. The sample was sputter-milled at low incident angle (17°) to remove both the $SiO_2$ substrate and the top Ni layer. Top: Low magnification micrographs of mainly Al layer, with some $NiAl_3$ grains (dark, irregularly shaped) evident in certain areas. Bottom: High magnification micrograph of an $NiAl_3$ grain in the Al matrix, and selected area diffraction (SAD) pattern of the same area. The pattern is indexed as $NiAl_3$ (Ref. 10).

annealed sample (324 °C, 80 min; see Fig. 8 for the BS spectrum) by ion milling at low incident angle (17°) first from one side to remove the $SiO_2$ substrate and then from the other side to remove the top Ni layer. Figure 9 contains both a bright-field micrograph and an electron diffraction pattern of this sample. Many $NiAl_3$ grains, as identified by the electron diffraction pattern,[10] are imbedded in an Al matrix, covering roughly 20%–30% of the area. This result indicates that at least a large fraction, if not all, of the Ni buried in Al has reacted with Al to nucleate $NiAl_3$.

A separate group of samples was contaminated in a different way. Instead of contaminating the original Al/Ni interface, a "dirty" interface is introduced halfway into the Al layer. The Al evaporation was interrupted after using up the Al source in one hearth, and resumed with Al in a second hearth. Such a procedure may result in a barrier at the interface of the two Al layers, and may also introduce uncontrolled impurities into the Al film as a whole. As exemplified in Fig. 10, the reaction upon furnace annealing behaves somewhat similarly to that of samples with a contaminated original Al/Ni interface (Fig. 8), except that now (i) the $NiAl_3$ step can be seen from the initial stage of reaction at the Al/Ni interface which is now presumably clean and (ii) Al penetration into Ni is insignificant. Figure 11 is a typical XTEM bright-field image of the reacted samples. Protrusions of big $NiAl_3$ grains into Al, localized mostly at Al grain boundaries, are evident. Presumably a very similar cross-sectional feature also prevails in samples with a contaminated original Al/Ni interface. The TEM observations described in this section lead us to conjecture that the Ni tail inside Al described in Sec. III B for contaminated Al is also composed largely of local $NiAl_3$ grains.

Once again, RTA at elevated temperatures for short durations ameliorates the nonuniformity at the Al/$NiAl_3$ interface for samples described in the last paragraph. The BS spectra of samples after RTA resemble those shown in Fig. 1. An example is shown in Fig. 12 (see Fig 10 for contrast). Samples with a contaminated original interface improve less. The $NiAl_3$ step has slanted edges and a small tail persists. Nevertheless, the highly nonuniform feature seen in Fig. 8 is no longer dominant.

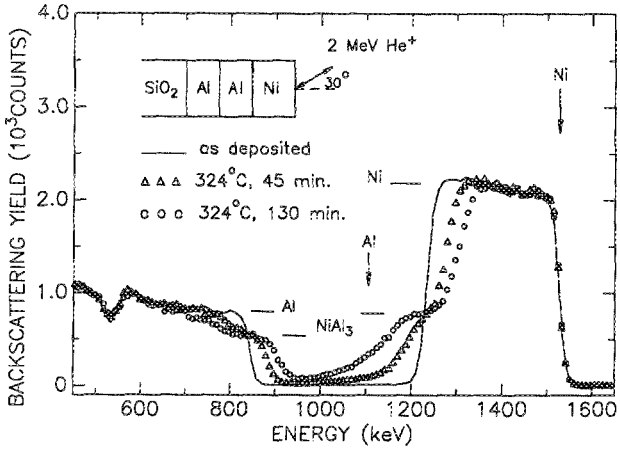


FIG. 10. 2-MeV $^4He^+$ backscattering spectra for Al/Ni samples with interrupted Al deposition (see insert for the as-deposited sample). The Al/$NiAl_3$ interface is nonuniform.

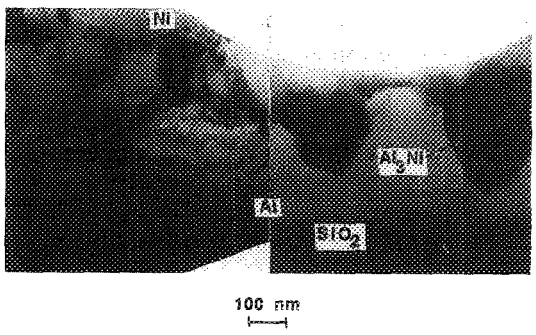


FIG. 11. Cross-sectional TEM bright-field image of the Al/Ni sample in Fig. 9 (324 °C, 130 min). Severe protrusions of $NiAl_3$ grains into the Al layer is evident.

As a result of the very rough Al/$NiAl_3$ interface, precise $NiAl_3$ growth kinetics cannot be extracted from BS spectra of the samples described in this section (III D). Nonetheless, by comparing Figs. 8 and 10 with Figs. 1 and 6, it is easy to tell that reactions in these samples progress slower than in the samples described in preceding sections (III A–III C). Roughly, the expansion of the reacted region ($NiAl_3$ step plus slanted tail) in the samples of Fig. 10 proceeds in a diffusion-limited fashion with a reaction constant that is about one-seventh of that of clean samples (Fig. 1).

## IV. DISCUSSION

### A. Comparison with previous data

In the first study of the Al/Ni thin-film reaction published in 1976,[6] Baglin and d'Heurle observed irregular growth of $NiAl_3$. Their BS spectra show slanted edges and scanning electron microscopy reveals a rough sample surface. The reaction was depicted as a two-stage process. Individual $NiAl_3$ grains grow first preferentially along Al grain boundaries, sustained by Ni diffusion. These grains later join to form a continuous $NiAl_3$ layer which grows further with a rough Al/$NiAl_3$ interface. The growth constant $k$ we estimate from their BS spectra is around $2\times10^{-15}$ cm$^2$/s at 275 °C. This value is more than one order of magnitude low-

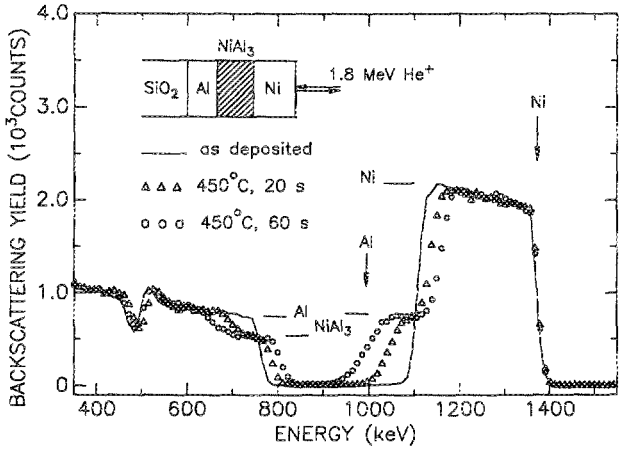


FIG. 12. 1.8-MeV $^4He^+$ backscattering spectra of $NiAl_3$/Ni samples with interrupted Al deposition (same as in Figs. 10 and 11) after RTA at 450 °C. The nonuniformity at the Al/$NiAl_3$ interface is improved. The $^4He^+$ beam is incident normal to the sample surface and the detection angle is 170°.

er than that expected from Fig. 4 for our clean samples, and is also lower than the rates found in our contaminated samples. This fact, as well as the resemblance between the reaction behaviors of their samples and of ours shown in Figs. 10 and 11 in Sec. III D, lead us to conjecture that some sort of contamination was probably involved in this early experiment.

Irregular behavior was also observed in a more recent experiment by Zhao *et al.*[5] As mentioned in Sec. III B, we have closely reproduced their results in our samples with a contaminated Al film. We note at this point that all the irregular features observed so far show up concomitantly with a pronounced reduction in the $NiAl_3$ growth rate as compared with clean samples (see the kinetics in Fig. 4). In contrast, our estimation from the published figures[7,8(b)] shows that the uniform layer-by-layer growth of $NiAl_3$ observed by Colgan, Nastasi, and Mayer possesses a growth constant close to 80% of that of our clean samples at 324 °C.

Therefore, in this work we have in fact recaptured qualitatively the various behaviors so far seen in Al-Ni thin-film reactions. The combined results suggest that the irregular $NiAl_3$ growth with typical features such as a rough Al/$NiAl_3$ interface, apparent Ni penetration into Al, and concurrent reduction of $NiAl_3$ growth rate, is not due to the effect of Al grain boundaries alone, but requires the presence of impurities. We cannot yet ascertain that contamination alone can lead to irregular reaction, as data on impure single-crystal or large-grained Al substrate are nonexistent. Our current results do suggest, though, that Al grain boundaries have a role in assisting the nonuniform penetration.

### B. $NiAl_3$ growth in contaminated samples

Before discussing the nonuniformities at the interfaces, we notice that in contaminated samples the $NiAl_3$ layer always grows at a reduced rate, but still proceeds via a transport-limited process characterized by a square-root time dependence. The exception to this is perhaps the case of a contaminated initial interface, where a physical barrier suppresses the compound formation, leading to interpenetration of Al and Ni that defies a characterization of time dependence. Up to this point we have not identified impurity species present in our samples. When searching for light gaseous impurities using AES profiling, we were unable to find detectable amounts of oxygen and carbon, which we believe to be the most probable candidates, inside the samples before and after annealing. This result suggests either that we have missed the principal impurity, or that a minute amount of oxygen and/or carbon below the AES detection limit (1–2 at. %) is sufficient to markedly alter the Al-Ni reaction behaviors. It is known that an impurity content of 1–2 at. % can indeed appreciably reduce the reaction rate in some Si-metal[13–15] as well as Al-metal diffusion couples.[5,17–19] Segregation of impurities into a thick, high concentration layer is unlikely in our case, because all the Al film can be consumed to form $NiAl_3$ upon prolonged annealing. A very thin layer with accumulated impurities, if present at interfaces for example, would not be detectable by AES, especially when a smear-out effect may exist during sputter profiling. Exactly which impurity species to blame is uncertain at present. In the following modeling, we have selected oxygen as the representative impurity since it is ubiquitous and since the general picture will not be altered by invoking other impurities. At the low annealing temperatures, oxygen is most likely to be immobile in the Al layer where it forms strong Al-O bonds. Oxygen introduced into Ni is also known to be immobile in our temperature range as shown by Scott.[13] The effect of oxygen is therefore largely predictable based on a model proposed in Refs. 13 and 14. We will see in the following discussion that the addition of oxygen either in the Al or the Ni layer can indeed slow down the growth of $NiAl_3$, while the transport of the dominant moving species remains rate limiting.

It is known that Al dominantly moves during uniform $NiAl_3$ growth.[7,20] In a diffusion couple, steady-state growth of a compound interlayer controlled by transport of a dominant moving species can be represented by the following equation[21]:

$$\frac{dx}{dt} \sim j = \frac{\Delta C D}{x}, \tag{1}$$

where $j$ is the flux of Al, $x$ is the thickness of the growing compound, $t$ is the annealing time, $D$ is the chemical interdiffusion coefficient, and $\Delta C$ is the concentration gradient of the moving species across the $NiAl_3$ compound layer, which, in our case, is Al. In integrated form, Eq. (1) becomes

$$x^2 \sim \Delta C D t. \tag{2}$$

Hence, the growth constant $k$ obtained experimentally (see Fig. 2) is determined by the product of $D$ and $\Delta C$. The observed decrease in $NiAl_3$ growth rate, therefore, must be associated with a corresponding reduction in $D$ and/or $\Delta C$.

Consider first the case when $D$ is affected. When oxygen is introduced into the stationary Ni layer, the immobile oxygen will be incorporated later in the growing $NiAl_3$ layer. This incorporation retards the Al transport through the compound layer, thereby reducing $D$ and consequently decreasing the growth rate. These events are indeed observed in our experiments (see Sec. III C). The growth constant decreases by only 10%–20%, which is a typical magnitude of reduction for moderate concentration of immobile impurities. This scenario is analogous to the case of immobile oxygen in Si during $NiAl_3$ formation. An oxygen concentration on the order of 1 at. % inside stationary Si reduces the $Ni_2Si$ growth rate insignificantly.[13]

Consider next the case when $\Delta C$ is affected. If oxygen is initially introduced into the Al layer, the oxygen is unlikely to diffuse into the growing $NiAl_3$ layer since oxygen and Al are strongly bonded and the diffusivity of an Al-O omplex should be much less than that of Al in $NiAl_3$. Oxygen thus accumulates in the neighborhood of the Al/$NiAl_3$ interfaces as Al leaves to diffuse across the compound layer. $D$ hence remains unaffected. In this case, an observed rate reduction must be due to a decrease in $\Delta C$. That decrease can be made possible by a drop of the Al concentration at the $NiAl_3$ boundary as being in local equilibrium with a thin oxygen-enriched layer resulting from oxygen accumulation. This picture can explain the observed reduction in growth rate reported in Sec. III B for a contaminated Al layer. However, none of our XTEM micrographs revealed an impurity-en-

riched layer at the Al/$NiAl_3$ interfacial region. If it indeed exists, such a layer must thus be very thin. We note that there is no inconsistency between the described oxygen accumulation and the inability to detect oxygen inside the film by AES. If we assume an initial 1-at.% uniform oxygen distribution introduced into Al, an estimate shows that the amount of oxygen accumulated at the interface after the consumption of 150-nm Al suffices to form the equivalent of $\sim 1.5$ nm of pure $Al_2O_3$. We have shown in Sec. III D that an interfacial impurity layer thinner than the native oxide and undetectable by AES profiling can cause drastic changes in the reaction.

In addition to the reduction in $NiAl_3$ growth rate, severe nonuniformity is observed in samples with contaminated Al or contaminated interface (Secs. III B and III D). In these cases, the fact that the $NiAl_3$/Ni interface remains sharp when Ni penetrates in Al on the other side of the compound is a proof that Ni is also participating in long-range mass transport. To substantiate this claim requires a marker experiment.[20,22] In a sense, the $NiAl_3$ compound layer can be regarded as a marker layer. The appearance and increase of Ni in the Al layer, mainly in the form of penetrating $NiAl_3$ grains, indicates that Ni moves with respect to the Al inside the Al layer. When a continuous $NiAl_3$ layer is absent, e.g., as a result of interface contamination that suppresses $NiAl_3$ formation (Sec. III D), Ni motion in Al may well become the dominant process, as evidenced in Fig. 8 and Refs. 5 and 6. Presumably Ni is moving along fast diffusion paths, i.e., Al grain boundaries, and remains there as a result of practically zero solubility of Ni in Al,[16] forming $NiAl_3$. Similar situations have been noted in some Al-metal thin-film reactions.[1,23] Once a continuous $NiAl_3$ layer is established, the Ni flux across the $NiAl_3$ layer should be insignificant since a previous marker experiment in uncontaminated samples indicates that the Ni flux through the uniform $NiAl_3$ layer is only 1/30 of that of Al (error bar 1/19 to 1/62).[1,20] The Al flux decreases in our contaminated samples, which probably enhances the role of Ni diffusion. In our current experiment, we cannot tell whether the Ni observed inside the Al layer indeed comes from a finite Ni flux through the $NiAl_3$ layer or from nonuniform dissociation of $NiAl_3$ at the Al/$NiAl_3$ interface. The appearance of a rough Al/$NiAl_3$ interface suggests that the atomic fluxes and the reaction at this interface are laterally nonuniform, giving rise to localized protrusions of $NiAl_3$ at preferred sites. It is not clear exactly how such penetrations are promoted by the presence of impurities in Al. The available evidence points toward a complex interplay of several mechanism which cannot be identified unequivocally from the present data.

The Al grain boundaries seem to provide pathways for an irregular reaction. As demonstrated in our previous work,[4,5] the use of large-grained Al substrates simplifies the reaction behavior by eliminating both Al grain boundaries and contamination inside the Al, provided the interface cleanliness is taken care of properly.

### C. The role of RTA

The beneficial effect of RTA in suppressing $NiAl_3$ protrusions in Al has been shown for all types of our samples. As we pointed out above, the Ni penetration in Al originates from Ni transport along short-circuit diffusion paths at the expense of layer-by-layer $NiAl_3$ growth. The former process, typically characterized by a low activation energy and hence a weak temperature dependence,[24] is favored at relatively low temperatures. At elevated temperatures such a process tends to be overshadowed by compound nucleation and growth which has a comparatively strong temperature dependence. Our work provides a successful example of promoting a desired process by RTA, one of its advantages being the ability to select among competing processes in a controllable manner.[25]

## V. CONCLUDING REMARKS

We have performed a systematic study on the growth of the first aluminide in an Al-Ni system, $NiAl_3$, during thermal annealing of a Ni film with evaporated Al substrates. A uniform layer-by-layer growth of $NiAl_3$ with diffusion-limited kinetics is observed. The same results have been reported for a Ni film evaporated on large-grained Al substrates in our previous work.[4,5] A single kinetics law applies for both types of Al substrates for the temperature range 250–400 °C.

The influence of contamination during sample preparation on reaction behaviors has also been systematically investigated. An irregular reaction, which refers to significant Ni penetration into Al, a rough Al/$NiAl_3$ interface with protruding $NiAl_3$ grains into Al, plus accompanying reduction in $NiAl_3$ growth rate, appears to correlate closely with two key factors: contamination and the presence of Al grain boundaries. The reaction, in general, is very sensitive to a minute amount of impurities. Contamination of either Ni or Al or the interface, in that order, results in an increasingly appreciable reduction of the reaction rate. Contamination of Al or the interface, probably combined with the presence of Al grain boundaries, causes a pronounced laterally irregular behavior.

Approaches to alleviate or eliminate the irregular behavior include careful control of sample preparation, use of single-crystal or large-grained Al, and rapid thermal processing. This study shows an interesting model case of interplay between intrinsic microstructure, extrinsic contamination, and subsequent processing method.

## ACKNOWLEDGMENTS

The authors wish to thank Professor W. L. Johnson of Caltech for helpful discussions on the results and on the general topic of reactions in thin-film diffusion couples, and Dr. E. Colgan of IBM East Fishkill for useful comments and suggestions. We appreciate the technical assistance of G. Mendenilla and K. Olver of Martin Marietta Laboratories. This work is supported at Caltech in part by the National Science Foundation-MRG Grant No. DMR-8811795 and by a grant from Intel Corporation.

[1]For a recent review, see E. G. Colgan and J. W. Mayer, Mater. Res. Soc. Symp. Proc. **119** (1988).
[2]D. Pramanik and A. N. Saxena, Solid State Technol. **26**, 127 (1983).

[3]J. E. E. Baglin and J. M. Poate, in *Thin Films-Interdiffusion and Reactions*, edited by J. M. Poate, K. N. Tu, and J. W. Mayer (Wiley, New York, 1978), Chap 9.
[4]X.-A. Zhao, E. Ma, and M-A. Nicolet, Mater. Lett. **5**, 200 (1987).
[5]X.-A. Zhao, H.-Y. Yang, E. Ma, and M-A. Nicolet, J. Appl. Phys. **62**, 1821 (1987).
[6]J. E. E. Baglin and F. M. d'Heurle, in *Ion Beam Surface Layer Analysis*, edited by O. Meyer, G. Linker, and F. Käppeler (Plenum, New York, 1976), Vol. 1, p. 385.
[7]E. G. Colgan, M. Nastasi, and J. W. Mayer, J. Appl. Phys. **58**, 4125 (1985).
[8](a) J. C. Liu, J. C. Barbour, and J. W. Mayer, Mater. Res. Soc. Symp. Proc. **108** (1988); (b) J. C. Liu, J. W. Mayer, and J. C. Barbour, J. Appl. Phys. **64**, 651 (1988).
[9]A. Katz and Y. Komem, E-MRS Symp. A Proc. (in press).
[10]JCPDS File No. 2-416 (OP16, *Pnma*).
[11]W. B. Pearson, *A Handbook of Lattice Spacings and Structures of Metals and Alloys* (Pergamon, Oxford, 1967), Vol. 2.
[12]X.-A. Zhao, T. C. Banwell, and M-A. Nicolet, SPIE **623**, 225 (1986).
[13]D. M. Scott, Ph. D. thesis, California Institute of Technology, 1982; also D. M. Scott and M-A. Nicolet, Nucl. Instrum. Methods **182/183**, 655 (1981).
[14]C.-D. Lien and M-A. Nicolet, J. Vac. Sci. Technol. B **2**, 738 (1984).
[15]G. Ottaviani, Thin Solid Films **140**, 3 (1986).
[16]T. B. Massalski, Ed., in *Binary Alloy Phase Diagrams* (American Society for Metals, Metals Park, OH, 1986), Vol. 1, p. 140.
[17]M. Wittmer, F. Le Goues, and H.-C. W. Huang, J. Electrochem. Soc. **132**, 1450 (1985).
[18]J. Tardy and K. N. Tu, Phys. Rev. B **32**, 2070 (1985).
[19]R. K. Nahar, N. M. Devashrayee, and W. S. Khokle, J. Vac. Sci. Technol. B **6**, 880 (1988).
[20]E. G. Colgan and J. W. Mayer, Nucl. Instrum. Methods Phys. Res. B **17**, 242 (1986).
[21]See, for example, U. Gösele and K. N. Tu, J. Appl. Phys. **53**, 3252 (1982).
[22]E. G. Colgan and J. W. Mayer, J. Mater. Res. **1**, 786 (1986).
[23]R. F. Lever, J. K. Howard, W. K. Chu, and P. J. Smith, J. Vac. Sci. Technol. **14**, 158 (1977).
[24]P. G. Shewmon, in *Diffusion in Solids* (McGraw-Hill, New York, 1963), Chap. 6.
[25]R. Singh, J. Appl. Phys. **63**, R59 (1988).